water

MDPI

Article

The Suitability of Pozzolan as Admixing Aggregate for Fe^0-Based Filters

Arnaud Igor Ndé-Tchoupé [1], Suzanne Makota [1], Achille Nassi [1], Rui Hu [2] and Chicgoua Noubactep [3,4,*]

1 Department of Chemistry, Faculty of Sciences, University of Douala, Douala BP 24157, Cameroon; ndetchoupe@gmail.com (A.I.N.-T.); s.makota@laposte.net (S.M.); achillen@yahoo.fr (A.N.)
2 School of Earth Science and Engineering, Hohai University, Fo Cheng Xi Road 8, Nanjing 211100, China; rhu@hhu.edu.cn
3 Department of Applied Geology, University of Göttingen, Goldschmidtstraße 3, Göttingen D-37077, Germany
4 Department of Water and Environmental Science and Engineering, Nelson Mandela African Institution of Science and Technology, Arusha 447, Tanzania
* Correspondence: cnoubac@gwdg.de; Tel.: +49-551-393-3191

Received: 6 March 2018; Accepted: 28 March 2018; Published: 2 April 2018

Abstract: Continuous gravity-fed column experiments using the methylene blue (MB) discoloration method were performed to characterize the suitability of a pozzolan (PZ) specimen as alternative admixing aggregate for metallic iron filters (Fe^0-filters). Investigated systems were: (i) pure sand, (ii) pure PZ, (iii) pure Fe^0, (iv) Fe^0/sand, (v) Fe^0/PZ, and (vi) Fe^0/sand/PZ. The volumetric proportion of Fe^0 was 25%. The volumetric proportions of the Fe^0/sand/PZ system was 25/45/30. The initial MB concentration was 2.0 mg·L^{-1}, 6.0 g of Fe^0 was used, and the experiments lasted for 46 days. The individual systems were fed with 3.9 to 8.4 L (7.80 to 16.69 mg of MB) and were characterized by the time-dependent changes of: (i) the pH value, (ii) the iron breakthrough, (iii) the MB breakthrough, and (iv) the hydraulic conductivity. Results showed that the Fe^0/sand/PZ system was the most efficient. This ternary system was also the most permeable and therefore the most sustainable. The suitability of MB as a powerful operative indicator for the characterization of processes in the Fe^0/H_2O system was confirmed. The tested PZ is recommended as an alternative material for efficient but sustainable Fe^0 filters.

Keywords: aqueous corrosion; packed-bed filters; pozzolan; water treatment; zero-valent iron

1. Introduction

Large-scale use of granular metallic iron (Fe^0) for environmental remediation and water treatment started in 1994 with the publication of experimental works on the degradation of halogenated aliphatics [1–4]. In 2002, the US EPA designated the Fe^0-permeable reactive barrier as a standard remediation technology. In the meantime, Fe^0 filtration is regarded as an established technology for water treatment [5–8]. However, despite 25 years of intensive research, Fe^0 filtration is still in its infancy as controversial reports are available on mechanistic and design aspects of the technology [9–12]. Ulsamer [13] recently summarized the state-of-the-art designing approaches, culminating at the point that it is uncertain whether sand admixture is a blessing or a curse for Fe^0 filters. A science-based progress has been recently presented [14–16] demonstrating that sand admixture is even a prerequisite for sustainable (long-term efficient) Fe^0 filters [17–21].

Properly designing an Fe^0-based filter implies the careful consideration of a balance between at least five interdependent key factors to satisfactorily eliminate the contamination of concern: (i) an appropriately

reactive Fe^0 material, (ii) appropriate inert or reactive admixing agents (e.g., gravel, MnO_2, pumice, sand), (iii) appropriate granular mixtures (e.g., Fe^0/sand, Fe^0/pumice, Fe^0/sand/pumice) and corresponding mixing ratios (e.g., 25% Fe^0—vol/vol), (iv) an appropriate filter thickness, and (v) an appropriate water flow velocity. The efficiency of a filter depends mainly on the balance of Fe^0 intrinsic reactivity and filter permeability. For a filter to be efficient in the long term (longevity), all design factors should be carefully considered [13,22–25].

Sand and gravel are two highly conductive natural aggregates that are conventionally used to modify the hydraulic conductivity (permeability) of geotechnical systems. To achieve this aim, these aggregates are commonly sorted and/or mixed. Admixtures with less conductive aggregates like pumice or pozzolan have also been reported. Sand and gravel were accordingly first used in Fe^0 filters to enhance the permeability of PRBs, which should be approximately one order of magnitude higher than the surrounding soils [26]. Besides fixing the permeability of Fe^0 filters, sand was believed to save Fe^0 costs while enabling the satisfaction of width requirements [27–29]. However, the discussion has not properly considered the volumetric expansive nature of iron corrosion [30]. The volume of each iron oxide (V_{ox}) is larger than that of the parent Fe^0 (V_{iron}). The expansion coefficient $\eta = V_{ox}/V_{iron}$ takes values varying from 2.1 to 6.4, the lower values corresponding to anoxic conditions [31,32]. The consideration of η values alone shows that a pure Fe^0 filter (100% Fe^0) will clog long before Fe^0 is depleted (Fe^0 wastage). Calculations have shown that the most sustainable dual Fe^0/aggregate system should contain 25% Fe^0 [20]. To date, the most tested/used aggregate is sand [26,33,34].

At some locations around the world, sand is scarce and volcanic rocks (pozzolan, pumice) are abundant. Therefore, it is important to characterize the behavior of these materials as alternatives to sand for the construction of Fe^0 filters. Ideally, such characterization tests are performed under field relevant conditions (e.g., no acceleration) and for the long term (e.g., months) [25,35]. Recently, the methylene blue (MB) discoloration method was introduced and used to characterize several aspects of the operation of Fe^0/H_2O systems [20,21,36–39]. The MB discoloration method exploits the low adsorptive affinity of MB to iron corrosion products (FeCPs) to characterize the reactivity of Fe^0 in a filter [17,21,40,41]. In fact, the in situ generation of FeCPs which coats the admixing aggregates lowers the absorptive affinity of the whole system for MB. This shortens the experimental duration and makes MB a reactive indicator [18].

The present work is aimed at characterizing the Fe^0/pozzolan (PZ) system as a possible alternative to the conventional Fe^0/sand system while using the methylene blue (MB) discoloration method. The six following systems are investigated: (i) pure sand, (ii) pure PZ, (iii) pure Fe^0, (iv) Fe^0/sand, (v) Fe^0/PZ, and (vi) Fe^0/sand/PZ. The systems are mainly characterized by the extent of iron breakthrough, MB breakthrough and changes in the pH values. The results are comparatively discussed.

2. Materials and Methods

2.1. Solutions

2.1.1. Methylene Blue

Methylene blue (MB) is widely used as a model contaminant to characterize the suitability of various systems for water treatment [42]. The MB (from KEM LIGHT Laboratories PVT. LTD., Mumbai, India) used herein was of analytical grade, and was selected for its differential affinity to sand and iron oxides [36,41]. The working solution has a molar concentration of 5.35 µM (2.0 $mg{\cdot}L^{-1}$) and was weekly prepared by properly diluting a 1000-fold concentrated stock solution (2000 $mg{\cdot}L^{-1}$) using the tap water of the city of Douala. The pH value of the initial solution was 7.0. The used initial concentration (2.0 $mg{\cdot}L^{-1}$) was selected to approach the concentration range of natural waters (MB as model micro-pollutant) [36].

2.1.2. Iron

A standard iron solution (990 $\mu g{\cdot}mL^{-1}$) from Aldrich Chemical Company, Inc. (Milwaukee, WI, USA), was used to calibrate the spectrophotometer used for analysis. All other used chemicals were of analytical

grade. In preparation for spectrophotometric analysis, ascorbic acid was used to reduce Fe^{III} in solution to Fe^{II}. 1,10-Phenanthroline from ACROS Organics (Geel, Belgium) was used as reagent for Fe^{II} complexation prior to spectrophotometric determination. Other chemicals used in this study included L(+)-ascorbic acid, L-ascorbic acid sodium salt, and sodium acetate.

2.2. Solid Materials

Three granular materials were used in this study. Table 1 summarizes some of their characteristics.

Table 1. Size, source, and nature of the three tested materials. The main selection criterion was local availability.

Materials	Size	Source	Nature
Sand	315 µm–630 µm	Collected (SWR *)	Adsorbent
Pozzolan	315 µm–630 µm	Collected (SWR *)	Porous adsorbent
Fe^0	<630 µm	Donated (AC **)	Adsorbent's generator

* South West Region/Cameroon; ** Aciéries du Cameroun.

2.2.1. Metallic Iron (Fe^0)

The used Fe^0 material was donated by a Cameroonian company that deals with metallic iron, Aciéries du Cameroun (Douala, Cameroon). The material is available as fillings with a particle size < 630 µm. The elemental composition of the material as analyzed by X-ray fluorescence was: Mn: 0.62%; Si: 0.52%; Cu: 0.23%; Cr: 0.2%; Ni: 0.1%. The material was used without any pretreatment. Fe^0 was proven a powerful discoloration agent for MB with the particularity that discoloration agents are progressively generated in situ [43].

2.2.2. Sand

The used sand was a natural material from the Mungo River (Cameroon). Mungo sand was sieved and particles ranging between 315 and 630 µm were retained, rinsed with water, and then warmed in boiling water for about 3 h. The sand was further dried at 200 °C in an oven for 2.0 h and then allowed to cool at room temperature. This sand was not only used to build up the first (H_1) and third (H_3) layers of the investigated systems but was also mixed with Fe^0 to build the reactive zone (H_{rz}) of some of the investigated systems (Table 2). Sand was used because of its worldwide availability and its use as an admixing agent in Fe^0/H_2O systems [33,44].

Table 2. Overview of the experimental setup of the column experiments. H_{rz} is the reactive zone, while H_1 and H_3, respectively, represent the bottom and the top sand layers of the systems. This table particularly shows the composition of the reactive zone (RZ) of individual systems. Columns 1, 2, and 3 (pure materials) were reference systems. The operational conditions for the Fe^0/sand/PM (PM = pumice) system of Btatkeu-K et al. [21] are also given.

Column	Fe^0 (g)	Fe^0 (wt %)	Sand (g)	Sand (vol %)	PZ (g)	PZ (vol %)	H_{rz} (cm)	H_1 (cm)	H_3 (cm)
1	6.0	100	0.0	0.0	0.0	0.0	2.2	3.8	3.4
2	0.0	0.0	8.0	100	0.0	0.0	2.4	3.8	3.2
3	0.0	0.0	0.0	0.0	8.0	100	2.8	3.8	2.8
4	6.0	25	6.0	75	0.0	0.0	3.2	3.8	2.2
5	6.0	25	0.0	0.0	6.0	75	3.5	3.8	2.2
6	6.0	25	3.6	45	2.4	30	3.7	3.8	2.1
Column	**Btatkeu-K et al. [21]**								
	Fe^0 (g)	**Fe^0 (wt %)**	**Sand (g)**	**Sand (vol %)**	**PM (g)**	**PM (vol %)**	**H_{rz} (cm)**	**H_1 (cm)**	**H_3 (cm)**
Fe^0/sand	65.0	50.4	63.9	49.6	0.0	0.0	9.8	8.0	14.7
Fe^0/PM	65.0	73.0	0.0	0.0	24.1	27.0	11.0	8.0	13.5
Fe^0/sand/PM	65.0	60.0	31.6	29.2	11.7	10.8	11.0	8.0	13.5

2.2.3. Pozzolan

Used PZ (red) was a natural material from Limbe (South West Region, Cameroon). Limbe PZ was sieved and particles ranging between 315 and 630 μm were retained and pretreated in the same manner as sand (Section 2.2.2). A PZ sample was finely ground, homogenized, and average bulk composition determined using a Bruker's X-ray Diffraction D8-Discover (Billerica, MA, USA) instrument. The X-ray powder Diffraction (XRD) analysis revealed that the material was essentially made up of: SiO_2: 81.2%; Al_2O_3: 10.0%; K_2O: 3.6%; Fe_2O_3: 2.2%; CaO: 0.6%; TiO_2: 0.5%; BaO: 0.1%; MnO: 0.05%; ZrO_2: 0.02%; SrO: 0.02%; Rb_2O: 0.01%; ZnO: 0.01%. PZ was used to build up the reactive zone of Fe^0/PZ and Fe^0/sand/PZ systems. PZ was tested as an admixing agent because of its high porosity (up to 60%) which could serve as a reservoir for the in-situ-generated Fe corrosion products (FeCPs) [37]. PZ exhibits adsorptive properties as well [45,46].

2.3. Experimental Procedure

Column studies were carried out in a PET (poly-(ethylene terephthalate)) column with an inner diameter of 3.0 cm and a length of 11.5 cm. The columns were packed from the bottom to the top as follows: (i) a 3.8-cm sand layer (H_1); (ii) a reactive zone (H_{rz}, variable) made up of either Fe^0/sand (column 4), Fe^0/PZ (column 5), or Fe^0/sand/PZ (column 6) mixture; and (iii) an H_3 variable third sand layer. The used mass of Fe^0 was 6.0 g. The volume occupied by 6.0 g Fe^0 served as a unit for building the reactive zone (H_{rz}). The corresponding masses of sand and/or PZ are documented in Table 2. The first 1 cm at the top of the column was left free for the resting solution (Figure 1) and the total depth of material in the individual system was 9.2 ± 0.4 cm.

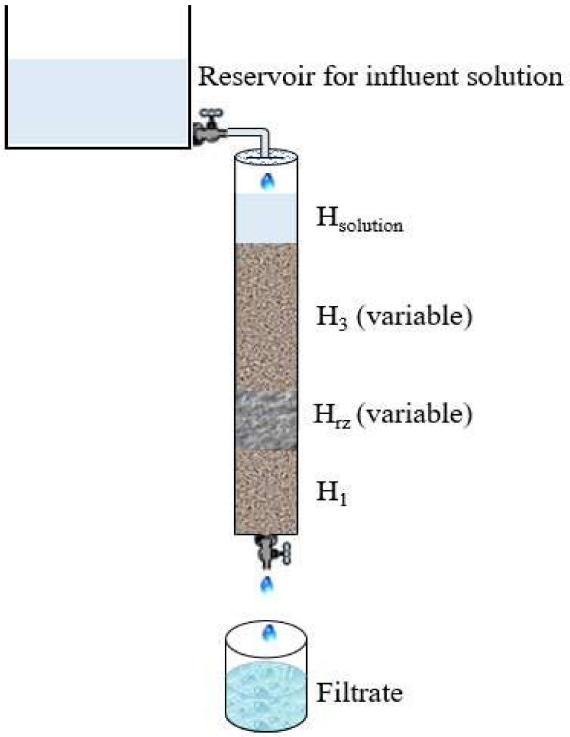

Figure 1. Schematic diagram of experimental setup. Due to the volumetric expansive nature of aqueous iron (Fe^0) corrosion, progressive permeability loss during use is expected.

A continuous gravity-driven filtration was performed through individual columns for 46 days. This experimental duration was not predetermined. The experiments were stopped mainly because the pure Fe^0 system was almost completely clogged. Filtration was initiated by percolating the working MB solution (2.0 $mg \cdot L^{-1}$) from a 500 mL bottle through each column. The MB solution was completed

daily to 500 mL. This approach mimics the situation where users will just have to refill the water tanks after a certain interval of time (here, one day) [47]. Previous investigations using gravity-fed systems filtered a constant volume daily [20,21]. This approach mimicked intermittent filtrations using household filters for daily water need in low-income communities. In the present approach, changes in flow velocity were observed through variations of the effluent volume. Effluents were collected daily and analyzed for MB and iron concentrations. The pH was also determined. The initial pH value of the MB working solution was 6.9 ± 0.2. Experiments were carried out at room temperature (28 ± 2 °C).

2.4. Analytical Methods

MB and aqueous iron concentrations were determined by a Spectroquant® pharo 300 UV-Vis spectrophotometer from Sigma-Aldrich Inc. (St. Louis, MO, USA). The working wavelength for MB was 664 nm. Dissolved iron was determined at 510 nm. Cuvettes with 1.0 cm light path were used. The iron determination followed the 1,10-Phenanthroline method [48]. The spectrophotometer was calibrated for MB concentrations $\leq$2.5 mg·L^{-1} and iron concentrations $\leq$10.0 mg·L^{-1}. The pH value was measured by combined glass electrodes (WTW Co., Weilheim, Germany).

2.5. Presentation of Experimental Results: E Values

In order to characterize the magnitude of tested systems for MB discoloration, the discoloration efficiency (E) was calculated using Equation (1). After the determination of the residual MB concentration (C), the corresponding percent MB discoloration was calculated as:

$$E(\%) = [1 - (C/C_0)] \times 100 \quad (1)$$

where C_0 is the initial aqueous MB concentration (2.0 mg·L^{-1}), while C gives the MB concentration at any date (t > 0).

In order to better characterize the effect of the tested materials on MB discoloration at the end of the experiment, two expressions of the specific discoloration efficiency (E_s and E_s^1) were calculated using Equations (2) and (3).

$$E_s = m_{discol}/m_{in} \times 100\% \quad (2)$$

$$E_s^1 = m_{rz}/m_{solid} \times 100\% \quad (3)$$

where m_{discol} is the MB mass discoloured within the column, m_{in} the total MB mass that has flowed through the column, and m_{solid} the mass of solid material present in the reactive zone. For the pure PZ and sand systems (0% Fe^0), m_{solid} corresponds to the total mass of material used. For Fe^0-based systems, m_{solid} corresponds to m_{Fe}. This simplification is rationalized by the assumption that sand and PZ in the reactive zone are covered by in-situ-generated iron corrosion products (FeCPs) while MB is quantitatively adsorbed onto H_3. It is also operationally assumed that H_1 (Table 2) does not significantly impact MB discoloration if significant flow disturbances happen in the reactive zone (H_{rz}) (assumption 1). The extent of MB discoloration (m_1 in mg) in the top sand layer (H_3) of individual columns was calculated from H_3 using the rule of proportion. In this effort, the pure sand system (0% Fe^0) was used as reference (9.4 cm of sand for 8.64 mg MB) (Equation (4)).

$$m_1(mg) = (H_3/9.4) \times 8.64 \quad (4)$$

Following assumption 1, the mass of MB discolored in H_{rz} is m_{rz}.

$$m_{rz}(mg) = m_{discol} - m_1 \quad (5)$$

3. Results and Discussion

3.1. Iron Release and pH Value

Figure 2 depicts the time-dependent changes of the dissolved iron concentration and the pH values in the effluents of the six investigated systems. Figure 2a summarizes the changes of the dissolved iron concentration in the effluents from the reference systems (0% Fe^0) and the four Fe^0-containing systems. It is seen that despite the fact that the systems contained the same mass of Fe^0 (6 g), different extents of iron release were obtained. The results could be summarized as follows: (i) no iron was released from the reference systems (sand and PZ), (ii) the lowest iron release (<3.4 mg· L^{-1}) was observed from the PZ-containing systems (Fe^0/PZ and Fe^0/sand/PZ), while (iii) the highest iron release (>3.4 mg·L^{-1}) was achieved in the PZ-free systems (100% Fe^0 and Fe^0/sand).

Figure 2b summarizes the results of the changes of the pH value in the six investigated systems. No significant changes in pH value could be observed. In fact, no clear trend in the pH evolution in all the systems was noticeable. All the systems depicted comparatively low pH values, close to the initial value (6.5). This could be attributed to acidification due to dissolution of SiO_2 [49]. The analytical results have demonstrated that used PZ is made up of 81.2% SiO_2. Sand was not analyzed but can be assumed to be pure SiO_2. The subsequent slight pH increase is attributed to iron corrosion. The most important feature from Figure 2b is that the pH value in all the investigated systems was larger than 6.0. It has been demonstrated elsewhere (Noubactep [50], and refs. cited therein) that in this pH range the solubility of iron is minimal. In fact, in Fe^0-based systems, the pH value significantly impacts the extent of Fe^0 dissolution. The migration of resulted Fe^{II} and Fe^{III} species within and out of the system also largely depends on the pH value. The fact that no significant changes in pH values were observed herein suggests that the observed difference with regard to the Fe concentration in the different systems (Figure 2a) can be attributed to meta-stable processes. In fact, the systems were relatively far from any equilibrium. In other words, the observed difference should be rationalized by two main arguments: (i) the adsorptive affinity of Fe^{II} and Fe^{III} species to the available materials and (ii) the system flow velocity (residence time). The retained increasing order of the extent of Fe release (Σm_{Fe} values in Table 3) in the Fe^0-based systems was: Fe^0/sand < Fe^0/PZ < 100% Fe^0 < Fe^0/sand/PZ. This classification is clearly related to the exact amount of Fe release by individual systems.

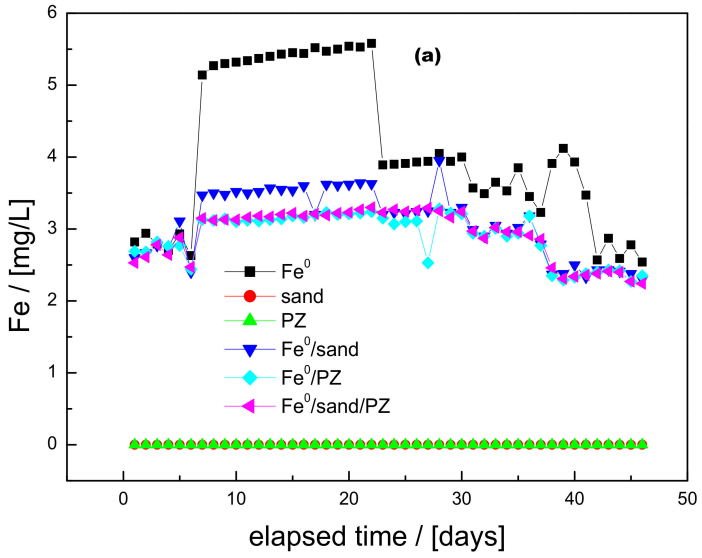

Figure 2. *Cont.*

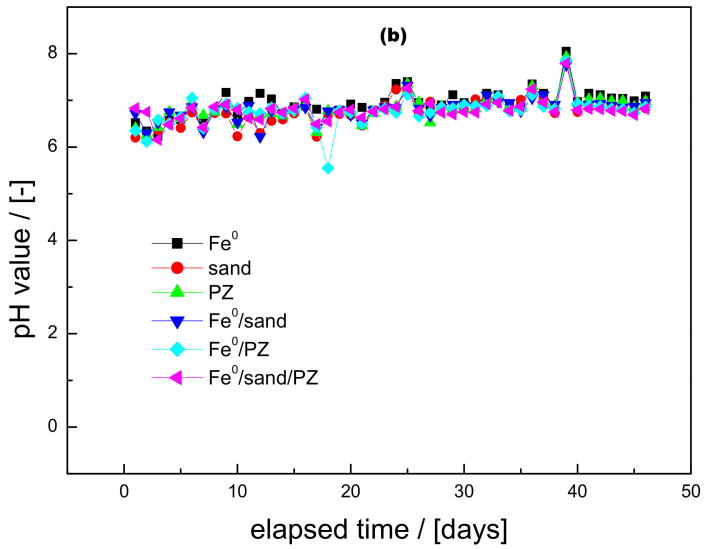

Figure 2. Time-dependent changes in effluent (**a**) iron concentration and (**b**) pH value for the 6 investigated systems. Experimental conditions: 6 g Fe^0; [MB] = 2.0 mg·L^{-1}. Filling materials: metallic iron (Fe^0), sand and pozzolan (PZ). Column length 11.5 cm; column diameter 3.0 cm. The lines are not fitting functions, they simply connect points to facilitate visualization.

Given that all the invested systems had the same fine sand at the bottom layer (H_1 = 3.8 cm), the observed difference can be attributed to processes occurring within the reactive zone (H_{rz}). Relevant processes include: (i) Fe^0 dissolution to Fe^{2+} and its oxidation to Fe^{3+}; (ii) the precipitation of Fe^{2+}/Fe^{3+} in the intergranular pore space; (iii) the adsorption of Fe^{2+}/Fe^{3+} onto solid surfaces such as Fe oxides, sand, and/or PZ; and (iv) the transport of Fe^{2+}/Fe^{3+} across the binary (Fe^0/sand or Fe^0/PZ) or ternary (Fe^0/sand/PZ) intermediate layer. Apart from the reference systems (including the 100% Fe^0 system), it can be seen from the cumulative residual Fe mass (Σm_{Fe}) in Table 3 that the released amount of Fe varied from 24.46 mg for the ternary Fe^0/sand/PZ system to 14.81 mg for the binary Fe^0/sand system.

Table 3. Summary of the column experiments results. V_T is the total volume of MB solution which flowed through individual columns. Σm_{Fe} and Σm_{MB} are, respectively, the effluent Fe and MB cumulative masses. m_1 and m_{rz} are calculated after Equations (4) and (5). E_s is the MB discoloration efficiency (Equation (2)) and $E_s{}^1$ the specific efficiency related to discoloration by H_{rz} and H_1. Results clearly show that PZ considerably enhances the sustainability of conventional Fe^0 filters.

Column	V_T (L)	m_{in} (mg)	Σm_{BM} (mg)	m_{discol} (mg)	Σm_{Fe} (mg)	m_1 (mg)	m_{rz} (mg)	E_s (mg·g^{-1})	$E_s{}^1$ (mg·g^{-1})
1	3.90	7.80	2.36	5.44	16.11	3.13	2.31	697.44	0.39
2	4.99	9.98	1.35	6.63	0.00	2.94	3.69	664.33	0.62
3	5.94	11.88	2.13	9.75	0.00	2.57	7.18	820.71	1.20
4	4.80	9.60	1.29	8.31	14.81	2.02	6.29	865.63	1.05
5	5.12	10.25	1.63	8.62	14.86	2.02	6.60	840.98	1.10
6	8.35	16.69	2.22	14.47	24.46	1.93	12.54	866.99	2.09

It is noticed that there was no significant difference between the amount of Fe released from the Fe^0/PZ system (column 5) and the Fe^0/sand system (column 4). The tiny difference (0.05 mg) renders also the argument with the residence time difficult. In fact, the time-dependent changes of the Fe concentration is very similar for both systems (Figure 2a). Therefore, given the similitude in particle size, it can be considered that the PZ porosity has limited impact on the system's behavior for the considered thickness of the reactive zone (RZ): 3.2 cm for Fe^0/sand and 3.5 cm for Fe^0/PZ (Table 2). Table 2 also recalls that the thickest RZ was the one with the ternary mixture (3.7 cm). Despite this tiny difference

in the extent of Fe release and considering the low amount of materials used, the fact that more Fe was released (absolute value) in the Fe^0/PZ system seems to negate the consideration that the pores of PZ have stored some iron corrosion products (FeCPs). However, whether they are interconnected or not, these pores exist and have certainly stored a part of FeCPs. Therefore, other arguments should be sought to rationalize these observations.

Compared to the Fe^0/sand system, less FeCPs precipitated in the vicinity of the Fe^0 surface in the Fe^0/PZ system. Accordingly, the generation of contaminant collectors was sustained [17–21]. However, the present work was performed with a smaller size Fe^0 material than the previous [17,18,21]. It is likely that this material was more reactive and the kinetics of its oxidative dissolution was such that despite storage of FeCPs in the PZ porous system, there is a larger excess dissolved Fe transported through H_{rz} and H_3 layers and detected in the effluent. Clearly, the combination of three factors satisfactorily explains the excess Fe release in the Fe^0/PZ system relative to the Fe^0/sand system. Because the PZ porosity cannot be negated, the size of the particles, the thickness of the columns, and the intrinsic reactivity of used Fe^0 rationalized the observations. This argument also rationalizes the behavior of the ternary systems (Fe^0/sand/PZ). In fact, when a fraction of PZ is substituted by sand, the permeability is increased (next section) and the transport of dissolved Fe facilitated. More Fe is released than in both binary systems (Fe^0/PZ and Fe^0/sand) (Figure 2a).

Iron species from Fe^0 oxidative dissolution in the reactive zone (H_{rz}, Figure 1) can only be released from the system if they succeed to migrate through the lower sand layer (H_1, Figure 1). The low solubility of iron for the investigated pH range (pH > 6.0) herein suggests that an in situ coating of this H_1-sand layer will occur through adsorption or adsorptive precipitation [17,51]. In the meantime, the removal of Fe by size exclusion or its adsorption onto aged Fe oxides within the H_{rz} layer or even its precipitation also occurs. In other words, the released Fe is the excess that has not interacted within the H_{rz} and H_1 layers.

The observation made for the two binary systems contrasts with the results of Btatkeu-k et al. [21] who reported more Fe released from the Fe^0/sand system while investigating the suitability of another porous additive (pumice). This can be rationalized by at least two main reasons: (i) the differences in the used Fe^0 type and size (intrinsic reactivity), and (ii) the differences in the operational conditions. While the investigations herein were done with a continuous filtration, Btatkeu-K al. [21] used an intermittent filtration. Moreover, the relative volumetric ratios of used materials are not identical in both studies (Table 2). Another minor argument is the evidence that pumice (PM) and PZ do not absolutely have the same physicochemical properties despite their highly porous nature. Another plausible explanation might be that the pores of PZ are more interconnected than those of PM (remark 1) such that coupled with continuous filtration, lesser residence time is offered in the PZ-containing systems. A lesser residence time means less time for Fe precipitation or high Fe breakthrough.

3.2. Hydraulic Conductivity

Figure 3 summarizes the results of the evolution of the effluent volume (V in mL) as a function of time for the six investigated systems. Herein, V values reflect the hydraulic conductivity. A monotone decrease of the V value is observed with the progress of the filtration (Figure 3a) in all systems. The decrease of V values in Fe^0-free systems is attributed to the progressive clogging due to accumulation of MB in the initial pore systems. Figure 3a also shows that while the initial V values for the Fe^0/sand, Fe^0/PZ, and the 0% Fe^0 reference systems were very close, the initial V value for the reference system (100% Fe^0) was the lowest and that of the ternary Fe^0/sand/PZ the highest. This behavior is primarily attributed to the initially available pore space in individual systems [52]. It should be kept in mind that PZ is a porous material. This explains why despite the similarity between the initial V values for the 0% Fe^0 (pure sand and pure PZ) reference systems, a close look at Figure 3a shows that the pure PZ system was a bit more permeable than the pure sand system. It is therefore intuitively considered that using the porous PZ to build the H_{rz} zone offers more open available pore spaces. This is true although the interconnectivity of pores is not explicitly addressed herein.

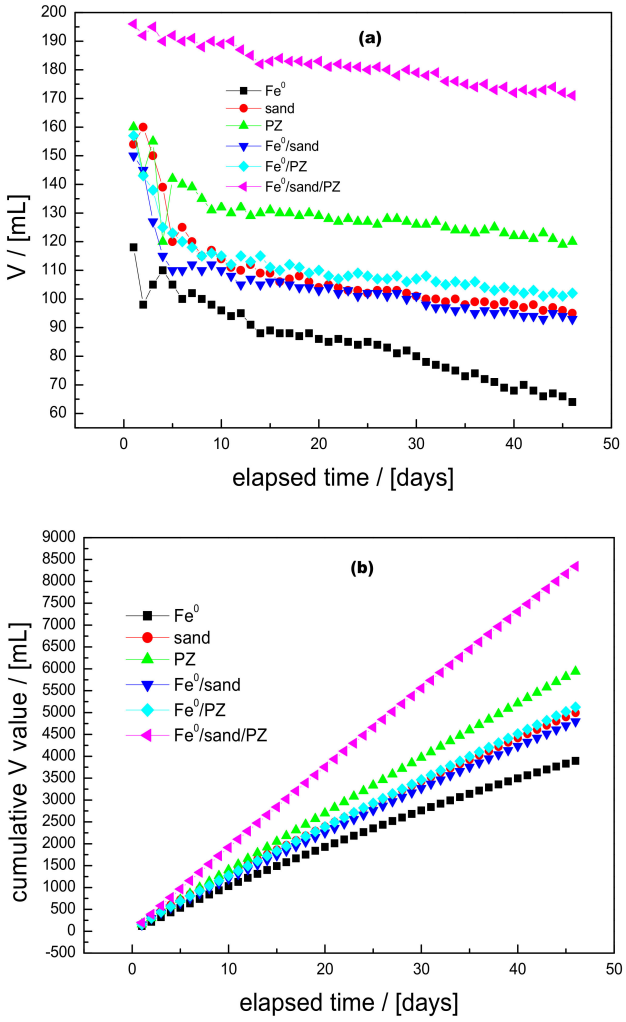

Figure 3. Time-dependent changes in effluent (**a**) volume and (**b**) cumulative volume for the 6 investigated systems. Experimental conditions: 6 g Fe^0; [MB] = 2.0 mg·L^{-1}. Filling materials: metallic iron (Fe^0), sand and pozzolan (PZ). Column length 11.5 cm; column diameter 3.0 cm. The lines are not fitting functions, they simply connect points to facilitate visualization.

The results presented in Figure 3b clearly demonstrate that the ternary Fe^0/sand/PZ system was the most permeable for the whole duration of the experiment. PZ thus enables the in situ control of expansive Fe^0 corrosion products which is the main cause of permeability loss. The above discussed close similarity between the permeability evolution of the Fe^0/PZ and Fe^0/sand is also confirmed. In fact, the cumulative effluent volumes at the end of the experiment (V_T in L—Table 3) are 5.12 L of the working solution filtered through the Fe^0/PZ system and 4.80 L for the Fe^0/sand system. The main information from the V_T values is that the PZ-containing systems were the most permeable. 5.94 L could be filtered through the pure PZ system and up to 8.35 L through the ternary Fe^0/sand/PZ. The decreasing order of sustained hydraulic conductivity was: Fe^0/sand/PZ > pure PZ > Fe^0/PZ > pure sand > Fe^0/sand > 100% Fe^0.

This shows that the least permeable system was the pure Fe^0 system (V_T = 3.90 L). This behavior is rationalized by the volumetric expansive nature of all Fe^0 particles in the H_{rz} zone (Figure 1) which has rapidly filled the initial interparticular porosity of the system [24,32]. The observed highest decrease in permeability for the 100% Fe^0 system is consistent with the observation of Hussam [53,54] that pure Fe^0 systems are efficient but not sustainable. This observation was the starting point for the manufacture of a proprietary porous iron composite in which the initial porosity leaves room for expansive iron

corrosion products [52]. The replacement of a fraction of Fe^0 by a nonexpansive material (e.g., gravel, sand, pumice) [14,55,56] was therefore found as an alternative approach.

The fact that a higher permeability is observed for the Fe^0/PZ system relative to the Fe^0/sand system is not sufficient to state whether the available pores are really interconnected. In fact, the observation that the ternary Fe^0/sand/PZ system is more conductive than the pure PZ system makes any attempt to conclude that there is a high degree of interconnectivity of available pores hardly acceptable. In other words, there are not enough available data herein to intensively discuss this aspect. It can be assumed that PZ pores have a certain percentage of interconnection. This explains why it was intuitively expected herein that the PZ-containing systems would exhibit greater permeability. In fact, testing another porous additive material (pumice), Bilardi et al. [18] have earlier reported an increased permeability of the Fe^0/PM system relative to the Fe^0/sand system, seemingly indicating that the enhancement of the sustainability of conventional Fe^0 filters can only be achieved via the utilization of porous additives in the reactive zone.

3.3. MB Discoloration

Figure 4 summarizes the results of MB discoloration (E values) in the six investigated systems. It is clearly seen that the 100% Fe^0 system was the least efficient at MB discoloration. It should be recalled that the 100% Fe^0 system was the least permeable system. This implies that the lowest MB volumes were daily filtered through this system. Accordingly, the observed rapid decrease of E values is attributed to (i) rapid generation of FeCPs filling the pore space and (ii) limited MB inflow due to system clogging. Hence, it is considered that the used Fe^0 material was a very reactive one. However, high reactivity is coupled with rapid efficiency loss due to rapid decrease of the hydraulic conductivity (efficient but not sustainable). In such a system, the small size of Fe^0 implies small pore size and hence rapid clogging [24,32].

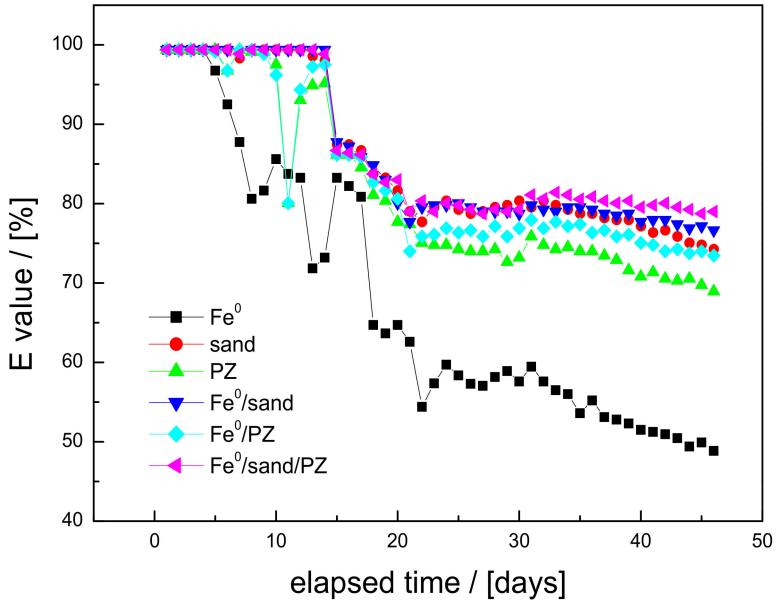

Figure 4. Time-dependent changes of methylene blue (MB) discoloration by the investigated systems. Experimental conditions: 6 g Fe^0; [MB] = 2.0 mg·L^{-1}. Filling materials: metallic iron (Fe^0), sand and pozzolan (PZ). Column length 11.5 cm; column diameter 3.0 cm. The lines are not fitting functions, they simply connect points to facilitate visualization.

The next less efficient system at MB discoloration is the pure PZ system. The low efficiency is rationalized by the fact that the system exhibited higher hydraulic conductivity compared to other systems apart from the Fe^0/sand/PZ system. In other words, the residence time was too short for quantitative MB discoloration. In fact, being close to sand in its mineralogical composition, PZ should be a good adsorbent for MB [20,36]. All the others systems exhibited greater but similar

trends in their discoloration efficiency. However, a meticulous observation shows, precisely towards the end of the experiment (t > 23 days), that the Fe^0/PZ system had a poorer efficiency compared to the Fe^0/sand system while the ternary system was remarkably the most efficient throughout the experimental duration. This observation is not totally confirmed by the m_{discol} values (Table 3) which represent the discolored MB masses within individual systems throughout the experimental duration. For instance, it is seen that while 8.62 mg of MB were discolored in the Fe^0/PZ system, 8.31 mg were instead discolored in the Fe^0/sand system and up to 14.47 mg were achieved in the Fe^0/sand/PZ system. This confirms the discussion in Section 3.1 while suggesting that PZ is a better MB discoloring agent than sand. This suggestion is supported by the data in Table 3 showing that 9.75 mg of MB were discolored in the pure PZ system and only 6.63 mg in the pure sand system. The fact that more MB was discolored in the Fe^0/sand/PZ system reflects an increased MB co-precipitation within the RZ by virtue of the accumulation of FeCPs in porous PZ.

Comparing the efficiency of the systems at MB discoloration on the basis of their various discoloration efficiency at the end of the experiment (E_s values) could be regarded as more realistic (than the m_{discol} values). The E_s values from Table 3 show that with 697.44 $mg \cdot g^{-1}$ the 100% Fe^0 system was the least efficient. The pure sand system (664.33 $mg \cdot g^{-1}$) exhibited a poorer efficiency compared to the pure PZ system (820.71 $mg \cdot g^{-1}$), the Fe^0/sand system (865.63 $mg \cdot g^{-1}$) was more efficient than the Fe^0/PZ system (840.98 $mg \cdot g^{-1}$), and the Fe^0/sand/PZ system with 866.99 $mg \cdot g^{-1}$ was the most efficient. This confirms observations already pointed out about the Fe^0/sand/PZ system regarding its efficiency at MB discoloration. Another important feature is that the higher available surface area is not available for the same experimental duration and the same hydraulic conductivity (different residence times). A discussion correlating the relative permeability and the effective surface of the systems is out of the scope of the present study. It is sufficient to acknowledge that the results herein confirm the fact that designing an efficient filter is concealing at least two antagonistic views: increased efficiency (higher surface area with PZ) and increased residence time (lower porosity but better drainage with sand) for the same hydraulic pressure (gravity) [18,19]. Another key factor to be considered is that iron corrosion is volumetrically expansive in nature. For the same additive (e.g., sand), one should find the balance between increased efficiency (more Fe^0—less sand) and increased permeability (less Fe^0—more sand). Btatkeu-K et al. [20] have experimentally demonstrated, using gravity-driven systems, that the optimal Fe^0 volumetric ratio for a sustainable Fe^0-based filter is 25%. Because the reasoning is based on the occupation of the initial porosity of the system, this result is universally valid, irrespective of the nature of the aggregates (Fe^0 and additives) [24].

The last important feature from Figure 4 is the comparison of the Fe^0/sand and the Fe^0/sand/PZ systems. As already pointed out, Fe^0/sand is the worst at discoloring MB. Figure 3 has shown that this system is also less permeable than the Fe^0/sand/PZ system. In the Fe^0/sand/PZ system, the porosity of PZ (larger adsorptive surface available) has favored a greater extent of precipitation of iron oxides within the H_{rz} layer. In other words, despite relative short residence time, increased adsorptive interactions with MB was possible in the ternary system. This has resulted in less Fe^{2+}/Fe^{3+}/MB competitions for adsorption onto H_1-sand and less coating H_1-sand with Fe oxides.

3.4. Discussion

The major output of this study is that the question of whether sand can be replaced by PZ can be affirmatively answered. However, the design effort is to optimize and to account for higher flow velocity and the degree of interconnectivity of PZ pores.

3.4.1. Significance of Results for the Design of Fe^0 Filtration Systems

The treatment efficiency of a Fe^0 bed is controlled by its initial porosity which is strongly influenced by material sorting, grain size and shape, and the used Fe^0 volumetric ratio in the material mixture [8,20,21,24,57–59]. Differences in grain size and grain morphology for Fe^0 and the additive material result in various degrees of compaction and thus various initial porosities [60,61]. Accordingly, the variation of effluent volume (V value) was used in this study to characterize

the evolution of the permeability (hydraulic conductivity). It is expected that future efforts to design Fe^0 household filters for the developing world will follow the protocol presented herein. The major advantage of this design is that water is continuously filtered and the filtered volume is known by the user. As soon as the filtered volume is lower than the daily use, the user should contact the provider. This direct feedback seems better that any electrical sensor. It should be explicitly stated that an efficient filter is sought, whether it is portable or not. Recent results from Heimann [62] using the MB method have confirmed previous observations that identical columns in series performed better than individual columns [25,63–65]. MB breakthrough was observed after 1 week from individual columns (duplicates) but there was no breakthrough after three weeks when two columns were operating in series. The results are rationalized by the O_2 scavenging function of the first column. The preferential flow created in the reactive zone and making H_3-sand useless for MB discoloration is eliminated in the tubing to column 2. It can be speculated that an efficient and sustainable Fe^0 household filter would comprise a slow sand filter and at least two Fe^0 columns. Maintenance could consist of periodically changing the first Fe^0 column (e.g., every two months). The path to efficient and sustainable Fe^0 filters goes exclusively through long-term experiments [25,66]. Ideally, experiments should run for at least six months, whether there is contaminant breakthrough or not. It is clear that upon complete clogging no experiment could be continued. It is therefore recommended to test only Fe^0 volumetric ratios lower than 40%. For comparability of published results, it would be better if the Fe^0 ratio is given in volumetric proportions. Alternatively, the densities and masses of all used aggregates should be specified.

3.4.2. The Service Life of Fe^0 Filters

Recent investigations have shown that the true problem of Fe^0 filters is the time-dependent loss of permeability [66–68]. According to Makota et al. [67], 'reactivity loss' is a mirage as it is just the natural decrease of the corrosion rate which is never a linear function of time [35]. In other words, if a proper material is selected, the major remaining task is to control the hydraulic conductivity (permeability).

Once an Fe^0 filter starts its operation ($t > t_0$), permeability loss starts as result of aqueous iron corrosion. The amount of in-situ-generated iron oxides (pore-filling cement) increases with increasing service life [32,69]. These iron oxides may also contribute to particle compaction (chemical compaction) and thus to pore occlusion. In the case of quantitative pore occlusion, the porosity of the system is reduced but the permeability is lost because of lack of interconnectivity. This process has been described in the entrance zone of Fe^0 beds working under toxic conditions [70]. In other words, both cementation and chemical compaction control the porosity of Fe^0 beds but compaction has the largest negative impact on permeability [59]. From this argument, it is clear the system exclusively made up of Fe^0 (pure Fe^0 bed or 100% Fe^0) will experience a more rapid permeability loss (Figure 3). This explains why the first-generation Fe^0 filters with 100% Fe^0 were mistakenly designed [53,54,71].

Figure 4 reveals that the most sustainable system (minimal permeability loss) is a ternary Fe^0/sand/PZ system. Figure 4 and the discussion in Section 3.3 also show that pure PZ systems are more sustainable and efficient at MB discoloration than pure sand systems. Meanwhile it has been intensively demonstrated that pure sand filters (biosand filters) just partly address biological contamination [72–76]. Amending biosand filters with Fe^0 is progressively established as an affordable and applicable alternative to more sophisticated systems [77,78]. The more important feature is that in-situ-generated ferrous and ferric oxides are contaminant collectors [17,19,36] besides impairing the permeability [20,24]. The question arises: which other type of non-expansive additive material could be added to an Fe^0/sand filter to enhance its sustainability and improve its efficiency to remove other relevant contaminants? The result achieved with PZ in this study has brought a reliable answer to this question and demonstrated that ternary systems such as the Fe^0/sand/PZ system are the most recommendable.

3.4.3. The Particularity of the Ternary Fe^0/Sand/PZ System

The evidence that the utilization of natural porous additives could be a blessing for the reported efficiency and permeability loss of conventional Fe^0 filters was first demonstrated by Moraci et al. [79,80]. Testing PM, Bilardi et al. [79] reported increased permeability of the Fe^0/PM system relative to the Fe^0/sand system but with a bit less treatability efficiency. Btatkeu-K et al. [21] therefore recently suggested that substituting a fraction of sand from the conventional Fe^0/sand by PM could yield an improved system (ternary system) concealing enhanced sustainability and maintained decontamination efficiency even though the results of their investigations finally contrasted with those of Bilardi et al. [79]. However, this contrast was rationalized by the differences in operational conditions, as the same 72% SiO_2-containing PM material was tested in both cases.

It should be noted that porous PZ tested in this study was essentially made up of SiO_2 (81.2%). This implies that as observed herein, while "PZ is an adsorbent as good as sand", it also clearly seems that "PZ is a better adsorbent than PM". This may also explain why combining PZ and sand yielded the most efficient system (Fe^0/sand/PZ) at MB discoloration. More importantly, as discussed in Section 3.1, the results of this study have also suggested that the pores of PZ are more interconnected than those of PM materials. This was rationalized by the fact that all the PZ-containing systems were the most conductive. This thus validates and consolidates the above report of Moraci et al. [79,80] but contradicts the results of Btatkeu-K et al. [21], suggesting that ternary Fe^0/sand/porous-additive systems would be less efficient and permeable than the conventional Fe^0/sand system. Meanwhile, the central rationale for testing the ternary Fe^0/sand/PM system by Btatkeu-K et al. [21] is confirmed in this study with the ternary Fe^0/sand/PZ system. This calls for more ample investigations on the Fe^0/sand/PM system with varied operational conditions for conclusive results. The very first step could be replicating the experiments reported herein with a larger amount of the same materials (e.g., 100 g Fe^0 and the corresponding amounts of PZ and sand). In the meantime, the achievement of this study and above discussion have clearly shown/confirmed that the ternary Fe^0/sand/PZ system is the best concealing long-term efficiency and enhanced sustainability.

4. Conclusions

The suitability of the MB method to characterize the reactivity of Fe^0-amended systems were confirmed. The results showed that the MB discoloration yields reliable data to understand processes occurring within the Fe^0-based systems (e.g., removal efficiency, permeability loss). The findings for the Fe^0/sand system were extended to the Fe^0/PZ and Fe^0/sand/PZ systems and enabled the characterization of the importance of using, as admixing aggregate to Fe^0 in the reactive zone, a material whose intrinsic porosity could serve as a reservoir for in-situ-generated FeCPs. This helps to delay Fe^0 'passivation' and hence to sustain its efficiency for a more sustainable filter. Results showed that PZ is such an appropriate admixing aggregate as all the PZ-containing systems appeared to be more sustainable and very efficient at MB discoloration. In particular, the Fe^0/sand/PZ system was optimal for concealing maximal MB discoloration and minimal permeability loss. This work confirmed the suitability of MB as a powerful operative indicator for the characterization of processes in the Fe^0/H_2O systems and confirms the hypothesis that porous additives are suitable for improving the sustainability of Fe^0 beds. It is expected that the results presented herein are used as a cornerstone to design the next generation of iron filters for use in households worldwide.

Acknowledgments: Thanks are due to Luc Mbaze Mva'a and Charles Kede (from the Department of Chemistry of University of Douala/Cameroon) for technical support and valuable advices. Lynne Beuleuk from the MIPROMALO (Mission of Local Materials Promotion) in Yaounde/Cameroon is also acknowledged for characterizing the materials tested in this study. The manuscript was improved by the insightful comments of anonymous reviewers from Water. We acknowledge support by the German Research Foundation and the Open Access Publication Funds of the Göttingen University.

Author Contributions: Arnaud Igor Ndé-Tchoupé conceived and designed the experiments which were validated by Suzanne Makota and Achille Nassi. Arnaud Igor Ndé-Tchoupé performed the experiments, analysed the results

and performed the literature review. The draft was written by Arnaud Igor Ndé-Tchoupé and Chicgoua Noubactep with contributions from Suzanne Makota, Achille Nassi and Rui Hu.

Conflicts of Interest: The authors declare no conflict of interest.

References

1. Lipczynska-Kochany, E.; Harms, S.; Milburn, R.; Sprah, G.; Nadarajah, N. Degradation of carbon tetrachloride in the presence of iron and sulphur containing compounds. *Chemosphere* **1994**, *29*, 1477–1489. [CrossRef]
2. Gillham, R.W.; O'Hannesin, S.F. Enhanced degradation of halogenated aliphatics by zero-valent iron. *Groundwater* **1994**, *32*, 958–967. [CrossRef]
3. Matheson, L.J.; Tratnyek, P.G. Reductive dehalogenationof chlorinated methanes by iron metal. *Environ. Sci. Technol.* **1994**, *28*, 2045–2053. [CrossRef] [PubMed]
4. Schreier, C.G.; Reinhard, M. Transformation of chlorinated organic compounds by iron and manganese powders in buffered water and in landfill leachate. *Chemosphere* **1994**, *29*, 1743–1753. [CrossRef]
5. Neumann, A.; Kaegi, R.; Voegelin, A.; Hussam, A.; Munir, A.K.M.; Hug, S.J. Arsenic removal with composite iron matrix filters in Bangladesh: A field and laboratory study. *Environ. Sci. Technol.* **2013**, *47*, 4544–4554. [CrossRef] [PubMed]
6. Ghauch, A. Iron-based metallic systems: An excellent choice for sustainable water treatment. *Freib. Online Geosci.* **2015**, *38*, 80.
7. Guan, X.; Sun, Y.; Qin, H.; Li, J.; Lo, I.M.C.; He, D.; Dong, H. The limitations of applying zero-valent iron technology in contaminants sequestration and the corresponding countermeasures: The development in zero-valent iron technology in the last two decades (1994–2014). *Water Res.* **2015**, *75*, 224–248. [CrossRef] [PubMed]
8. Mwakabona, H.T.; Ndé-Tchoupé, A.I.; Njau, K.N.; Noubactep, C.; Wydra, K.D. Metallic iron for safe drinking water provision: Considering a lost knowledge. *Water Res.* **2017**, *117*, 127–142. [CrossRef] [PubMed]
9. Noubactep, C. A critical review on the mechanism of contaminant removal in Fe^0–H_2O systems. *Environ. Technol.* **2008**, *29*, 909–920. [CrossRef] [PubMed]
10. Gheju, M. Hexavalent chromium reduction with zero-valent iron (ZVI) in aquatic systems. *Water Air Soil Pollut.* **2011**, *222*, 103–148. [CrossRef]
11. Noubactep, C. On the suitability of admixing sand to metallic iron for water treatment. *Int. J. Environ. Pollut. Solut.* **2013**, *1*, 22–36. [CrossRef]
12. Tepong-Tsindé, R.; Crane, R.; Noubactep, C.; Nassi, A.; Ruppert, H. Testing metallic iron filtration systems for decentralized water treatment at pilot scale. *Water* **2015**, *7*, 868–897. [CrossRef]
13. Ulsamer, S. A Model to Characterize the Kinetics of Dechlorination of Tetrachloroethylene and Trichloroethylene by a Zero Valent Iron Permeable Reactive Barrier. Master's Thesis, Worcester Polytechnic Institute, Worcester, MA, USA, 2011; p. 73. Available online: https://web.wpi.edu (accessed on 30 March 2018).
14. Noubactep, C.; Caré, S. Dimensioning metallic iron beds for efficient contaminant removal. *Chem. Eng. J.* **2010**, *163*, 454–460. [CrossRef]
15. Noubactep, C.; Caré, S. Designing laboratory metallic iron columns for better result comparability. *J. Hazard. Mater.* **2011**, *189*, 809–813. [CrossRef] [PubMed]
16. Noubactep, C.; Temgoua, E.; Rahman, M.A. Designing iron-amended biosand filters for decentralized safe drinking water provision. *Clean Soil Air Water* **2012**, *40*, 798–807. [CrossRef]
17. Bilardi, S.; Calabrò, P.S.; Caré, S.; Moraci, N.; Noubactep, C. Improving the sustainability of granular iron/pumice systems for water treatment. *J. Environ. Manag.* **2013**, *121*, 133–141. [CrossRef] [PubMed]
18. Miyajima, K.; Noubactep, C. Impact of Fe^0 amendment on methylene blue discoloration by sand columns. *Chem. Eng. J.* **2013**, *217*, 310–319. [CrossRef]
19. Miyajima, K. Optimizing the design of metallic iron filters for water treatment. *Freib. Online Geosci.* **2012**, *32*, 60.
20. Btatkeu-K, B.D.; Olvera-Vargas, H.; Tchatchueng, J.B.; Noubactep, C.; Caré, S. Determining the optimum Fe^0 ratio for sustainable granular Fe^0/sand water filters. *Chem. Eng. J.* **2014**, *247*, 265–274. [CrossRef]
21. Btatkeu-K, B.D.; Tchatchueng, J.B.; Noubactep, C.; Caré, S. Designing metallic iron based water filters: Light from methylene blue discoloration. *J. Environ. Manag.* **2016**, *166*, 567–573. [CrossRef] [PubMed]
22. Bartzas, G.; Komnitsas, K. Solid phase studies and geochemical modelling of low-cost permeable reactive barriers. *J. Hazard. Mater.* **2010**, *183*, 301–308. [CrossRef] [PubMed]

23. Li, L.; Benson, C.H. Evaluation of five strategies to limit the impact of fouling in permeable reactive barriers. *J. Hazard. Mater.* **2010**, *181*, 170–180. [CrossRef] [PubMed]
24. Domga, R.; Togue-Kamga, F.; Noubactep, C.; Tchatchueng, J.B. Discussing porosity loss of Fe^0 packed water filters at ground level. *Chem. Eng. J.* **2015**, *263*, 127–134. [CrossRef]
25. Simon, S.; Courtin-Nomade, A.; Vasiliu, A.; Sleiman, N.; Deluchat, V. Long-term influence of aeration on arsenic trapping in ZVI/sand bed reactor. *RSC Adv.* **2016**, *6*, 54479–54485. [CrossRef]
26. O'Hannesin, S.F.; Gillham, R.W. Long-term performance of an in situ "iron wall" for remediation of VOCs. *Groundwater* **1998**, *36*, 164–170. [CrossRef]
27. Song, D.-I.; Kim, Y.H.; Shin, W.S. A simple mathematical analysis on the effect of sand in Cr(VI) reduction using zero valent iron. *Korean J. Chem. Eng.* **2005**, *22*, 67–69. [CrossRef]
28. Bi, E.; Devlin, J.F.; Huang, B. Effects of mixing granular iron with sand on the kinetics of trichloroethylene reduction. *Groundw. Monit. Remed.* **2009**, *29*, 56–62. [CrossRef]
29. Henderson, A.D.; Demond, A.H. Impact of solids formation and gas production on the permeability of ZVI PRBs. *J. Environ. Eng.* **2011**, *137*, 689–696. [CrossRef]
30. Pilling, N.B.; Bedworth, R.E. The oxidation of metals at high temperatures. *J. Inst. Met.* **1923**, *29*, 529–591.
31. Caré, S.; Nguyen, Q.T.; L'Hostis, V.; Berthaud, Y. Mechanical properties of the rust layer induced by impressed current method in reinforced mortar. *Cem. Concr. Res.* **2008**, *38*, 1079–1091. [CrossRef]
32. Caré, S.; Crane, R.; Calabrò, P.S.; Ghauch, A.; Temgoua, E.; Noubactep, C. Modelling the permeability loss of metallic iron water filtration systems. *Clean Soil Air Water* **2013**, *41*, 275–282. [CrossRef]
33. Trois, C.; Cibati, A. South African sands as a low cost alternative solution for arsenic removal from industrial effluents in permeable reactive barriers: Column tests. *Chem. Eng. J.* **2015**, *259*, 981–989. [CrossRef]
34. Phukan, M.; Noubactep, C.; Licha, T. Characterizing the ion-selective nature of Fe^0-based filters using azo dyes. *Chem. Eng. J.* **2015**, *259*, 481–491. [CrossRef]
35. Noubactep, C. Predicting the hydraulic conductivity of metallic iron filters: Modeling gone astray. *Water* **2016**, *8*, 162. [CrossRef]
36. Miyajima, K.; Noubactep, C. Effects of mixing granular iron with sand on the efficiency of methylene blue discoloration. *Chem. Eng. J.* **2012**, *200*, 433–438. [CrossRef]
37. Ndé-Tchoupé, A.I. Designing Metallic Iron (Fe0)—Based Filters: Contribution to a Convenience Scale. Master's Thesis, University of Douala, Douala, Cameroon, 20 January 2015.
38. Tepong-Tsindé, R.; Phukan, M.; Nassi, A.; Noubactep, C.; Ruppert, H. Validating the efficiency of the MB discoloration method for the characterization of Fe^0/H_2O systems using accelerated corrosion by chloride ions. *Chem. Eng. J.* **2015**, *279*, 353–362. [CrossRef]
39. Gatcha-Bandjun, N.; Noubactep, C.; Loura Mbenguela, B. Mitigation of contamination in effluents by metallic iron: The role of iron corrosion products. *Environ. Technol. Innov.* **2017**, *8*, 71–83. [CrossRef]
40. Btatkeu-K, B.D.; Miyajima, K.; Noubactep, C.; Caré, S. Testing the suitability of metallic iron for environmental remediation: Discoloration of methylene blue in column studies. *Chem. Eng. J.* **2013**, *215*, 959–968. [CrossRef]
41. Mitchell, C.; Poole, P.; Segrove, H.D. Adsorption of methylene blue by high silica sands. *Nature* **1955**, *176*, 1025–1026. [CrossRef]
42. Avom, J.; Ketcha, J.; Noubactep, C.; Germain, P. Adsorption of methylene blue from an aqueous solution onto activated carbons from palm-tree cobs. *Carbon* **1997**, *35*, 365–369. [CrossRef]
43. Noubactep, C. Characterizing the discoloration of methylene blue in Fe^0/H_2O systems. *J. Hazard. Mater.* **2009**, *166*, 79–87. [CrossRef] [PubMed]
44. Varlikli, C.; Bekiari, V.; Kus, M.; Boduroglu, N.; Oner, I.; Lianos, P.; Lyberatos, G.; Icli, S. Adsorption of dyes on Sahara desert sand. *J. Hazard. Mater.* **2009**, *170*, 27–34. [CrossRef] [PubMed]
45. Kofa, G.P.; Ndi Koungou, S.; Kayem, G.J.; Kamga, R. Adsorption of arsenic by natural pozzolan in a fixed bed: Determination of operating conditions and modelling. *J. Water Process Eng.* **2015**, *6*, 166–173. [CrossRef]
46. Kofa, G.P.; Ndi Koungou, S.; Kayem, G.J.; Kamga, R. Kinetics and adsorption isotherms of arsenic (V) onto natural pozzolan. *J. Eng. Appl. Sci.* **2013**, *8*, 97–103.
47. Chiew, H.; Sampson, M.L.; Huch, S.; Ken, S.; Bostick, B.C. Effect of groundwater iron and phosphate on the efficacy of arsenic removal by iron-amended biosand filters. *Environ. Sci. Technol.* **2009**, *43*, 6295–6300. [CrossRef] [PubMed]
48. Fortune, W.B.; Mellon, M.G. Determination of iron with o-phenanthroline: A spectrophotometric study. *Ind. Eng. Chem. Anal. Ed.* **1938**, *10*, 60–64. [CrossRef]

49. Kaplan, D.I.; Gilmore, T.J. Zero-valent iron removal rates of aqueous Cr(VI) measured under flow conditions. *Water Air Soil Pollut.* **2004**, *155*, 21–33. [CrossRef]
50. Noubactep, C. Metallic iron for safe drinking water worldwide. *Chem. Eng. J.* **2010**, *165*, 740–749. [CrossRef]
51. Phukan, M. Characterizing the Fe^0/sand system by the extent of dye discoloration. *FOG* **2015**, *42*, 80.
52. Rahman, M.A.; Karmakar, S.; Salama, H.; Gactha-Bandjun, N.; Btatkeu-K, B.D.; Noubactep, C. Optimising the design of Fe^0-based filtration systems for water treatment: The suitability of porous iron composites. *J. Appl. Solut. Chem. Model.* **2013**, *2*, 165–177.
53. Hussam, A.; Munir, A.K.M. A simple and effective arsenic filter based on composite iron matrix: Development and deployment studies for groundwater of Bangladesh. *J. Environ. Sci. Health A* **2007**, *42*, 1869–1878. [CrossRef] [PubMed]
54. Hussam, A. Contending with a development disaster: SONO filters remove arsenic from well water in Bangladesh. *Innovations* **2009**, *4*, 89–102. [CrossRef]
55. Noubactep, C.; Caré, S.; Togue-Kamga, F.; Schöner, A.; Woafo, P. Extending service life of household water filters by mixing metallic iron with sand. *Clean Soil Air Water* **2010**, *38*, 951–959. [CrossRef]
56. Noubactep, C.; Caré, S.; Btatkeu-K, B.D.; Nanseu-Njiki, C.P. Enhancing the sustainability of household Fe^0/sand filters by using bimetallics and MnO_2. *Clean Soil Air Water* **2011**, *40*, 100–109. [CrossRef]
57. Carman, P.C. Fluid flow through granular beds. *Tran. Inst. Chem. Eng.* **1937**, *15*, 150–156. [CrossRef]
58. Salem, H.S.; Chilingarian, G.V. The cementation factor of Archie's equation for shaly sand stone reservoirs. *J. Pet. Sci. Eng.* **1999**, *23*, 83–93. [CrossRef]
59. Hubbe, M.A.; Chen, H.; Heitmann, J.A. Permeability reduction phenomena in packed beds, fiber mats, and wet webs of paper exposed to flow of liquids and suspensions: A review. *BioResources* **2009**, *4*, 405–451.
60. Dias, R.P.; Teixeira, J.A.; Mota, M.G.; Yelshin, A.I. Particulate binary mixtures: Dependence of packing porosity on particle size ratio. *Ind. Eng. Chem. Res.* **2004**, *43*, 7912–7919. [CrossRef]
61. Kubare, M.; Haarhoff, J. Rational design of domestic biosand filters. *J. Water Supply Res. Technol. Aqua* **2010**, *59*, 1–15. [CrossRef]
62. Heimann, S. Testing Granular Iron for Fluoride Removal. Master's Thesis, University of Göttingen, Göttingen, Germany, 2018. In Preparation.
63. Leupin, O.X.; Hug, S.J.; Badruzzaman, A.B.M. Arsenic removal from Bangladesh tube well water with filter columns containing zerovalent iron filings and sand. *Environ. Sci. Technol.* **2005**, *39*, 8032–8037. [CrossRef] [PubMed]
64. Avilés, M.; Garrido, S.E.; Esteller, M.V.; De La Paz, J.S.; Najera, C.; Cortés, J. Removal of groundwater arsenic using a household filter with iron spikes and stainless steel. *J. Environ. Manag.* **2013**, *131*, 103–109. [CrossRef] [PubMed]
65. Mehta, V.S.; Chaudhari, S.K. Arsenic removal from simulated groundwater using household filter columns containing iron filings and sand. *J. Water Process Eng.* **2015**, *6*, 151–157. [CrossRef]
66. Noubactep, C. Designing metallic iron packed-beds for water treatment: A critical review. *Clean Soil Air Water* **2016**, *44*, 411–421. [CrossRef]
67. Makota, S.; Nde-Tchoupe, A.I.; Mwakabona, H.T.; Tepong-Tsindé, R.; Noubactep, C.; Nassi, A.; Njau, K.N. Metallic iron for water treatment: Leaving the valley of confusion. *Appl. Water Sci.* **2017**, *7*, 4177–4196. [CrossRef]
68. Moraci, N.; Lelo, D.; Bilardi, S.; Calabrò, P.S. Modelling long-term hydraulic conductivity behaviour of zero valent iron column tests for permeable reactive barrier design. *Can. Geotech. J.* **2016**, *53*, 946–961. [CrossRef]
69. Noubactep, C. Metallic iron for water treatment: A critical review. *Clean Soil Air Water* **2013**, *41*, 702–710. [CrossRef]
70. Mackenzie, P.D.; Horney, D.P.; Sivavec, T.M. Mineral precipitation and porosity losses in granular iron columns. *J. Hazard. Mater.* **1999**, *68*, 1–17. [CrossRef]
71. Ngai, T.K.K.; Shrestha, R.R.; Dangol, B.; Maharjan, M.; Murcott, S.E. Design for sustainable development—Household drinking water filter for arsenic and pathogen treatment in Nepal. *J. Environ. Sci. Health A* **2007**, *42*, 1879–1888. [CrossRef] [PubMed]
72. Anderson, W. On the purification of water by agitation with iron and by sand filtration. *J. Soc. Arts* **1886**, *35*, 29–38. [CrossRef]
73. Devonshire, E. The purification of water by means of metallic iron. *J. Frankl. Inst.* **1890**, *129*, 449–461. [CrossRef]

74. Frechen, F.-B.; Exler, H.; Romaker, J.; Schier, W. Long-term behaviour of a gravity-driven dead end membrane filtration unit for potable water supply in cases of disasters. *Water Sci. Technol. Water Supply* **2011**, *11*, 39–44. [CrossRef]
75. Nitzsche, K.S.; Lan, V.M.; Trang, P.T.K.; Viet, P.H.; Berg, M.; Voegelin, A.; Planer-Friedrich, B.; Zahoransky, J.; Müller, S.-K.; Byrne, J.M.; et al. Arsenic removal from drinking water by a household sand filter in Vietnam—Effect of filter usage practices on arsenic removal efficiency and microbiological water quality. *Sci. Total Environ.* **2015**, *502*, 526–536. [CrossRef] [PubMed]
76. Feistel, U.; Otter, P.; Kunz, S.; Grischek, T.; Feller, J. Field tests of a small pilot plant for the removal of arsenic ingroundwater using coagulation and filtering. *J. Water Process Eng.* **2016**, *14*, 77–85. [CrossRef]
77. Erickson, A.J.; Gulliver, J.S.; Weiss, P.T. Phosphate removal from agricultural tile drainage with iron enhanced sand. *Water* **2017**, *9*, 672. [CrossRef]
78. Allred, B.J. Batch test screening of industrial product/byproduct filter materials for agricultural drainage water treatment. *Water* **2017**, *9*, 791. [CrossRef]
79. Bilardi, S.; Calabrò, P.S.; Caré, S.; Moraci, N.; Noubactep, C. Effect of pumice and sand on the sustainability of granular iron beds for the removal of CuII, NiII, and ZnII. *Clean Soil Air Water* **2013**, *41*, 835–843. [CrossRef]
80. Moraci, N.; Calabrò, P.S. Heavy metals removal and hydraulic performance in zero-valent iron/pumice permeable reactive barriers. *J. Environ. Manag.* **2010**, *91*, 2336–2341. [CrossRef] [PubMed]